LM-02K021
April 5, 2002

The Effects of Processing Parameters on Microstructure and Properties of Laser Deposited PM Alloy 690N_2 Powder

J.W. Sears

NOTICE

2002 International Conference on Metal Powder Deposition for Rapid Manufacturing
April 8-10, 2002
San Antonio, Texas

"The Effects of Processing Parameters on Microstructure and Properties of Laser Deposited PM Alloy $690N_2$ Powder"

by

James W. Sears, Lockheed Martin

ABSTRACT

Powder Metallurgy (PM) Alloy $690N_2$, the PM derivative of Inconel[1] 690 (IN 690), has been shown to have a higher elevated temperature yield strength and superior stress corrosion cracking (SCC) resistance than conventionally processed IN 690. The property improvements seen in Alloy PM $690N_2$ are due to interstitial nitrogen strengthening and precipitation hardening resulting from the formation of fine Titanium/ Chromium – nitrides. The application of Alloy PM $690N_2$ has had limited use due to the high costs involved in producing wrought products from powder. Laser Powder Deposition (LPD) offers another technique to take advantage of PM $690N_2$ properties.

Three different variations of the Alloy 690 chemistry have been deposited, PM chemistry – nitrogen atomized (PM $690N_2$), Ingot Metallurgy (IM) chemistry – nitrogen atomized (IM $690N_2$), and IM chemistry – argon atomized (IM 690Ar). The microstructural and mechanical property variations of these LPD deposited materials are reported. Alloy PM $690N_2$ powder was laser deposited at rates from .1 to over 12 cubic inches per hour at laser input powers ranging from 250 to 5000 watts using both CO_2 and Nd:YAG lasers. In all cases a fully dense material has been produced. There is a question however of how the properties of this material respond over such a wide range of parameters. An attempt has been made to correlate the processing conditions with the resultant microstructures and properties. The effects of LPD on the microstructural features and properties of Alloy PM $690N_2$ are discussed.

LASER POWDER DEPOSITION (LPD)

LPD is an extension of the laser cladding technology. A schematic of the LPD process is shown in Figure 1. LPD uses the concepts of laser cladding and applies them to the fabrication of prototype and functional components. Vilar[2] gives a comprehensive review of the laser cladding technology by explaining how

this technology has evolved into a viable industry. In laser cladding the heat-affected zone (HAZ) in the underlying surface is minimized, high-density coatings are produced, and the dilution of the clad into the substrate can be closely controlled. The laser cladding work coupled with the advent of Rapid Prototyping (RP) has led to the various efforts to form components by fusing metal powders[3].

LPD processing is performed by injecting powder into a small molten pool produced by a Nd:YAG or CO_2 laser. The motion of the laser over the underlying material is controlled through a computer interface. A design is digitally entered into a computer to produce a layer-by-layer representation of the desired product. The speed control of the laser (linear velocity), thickness of each layer, width step of each pass (hatch spacing), powder mass flow rate, and absorbed laser energy are key operating parameters. The control of the molten pool size is predominately influenced by the absorbed energy from the laser.

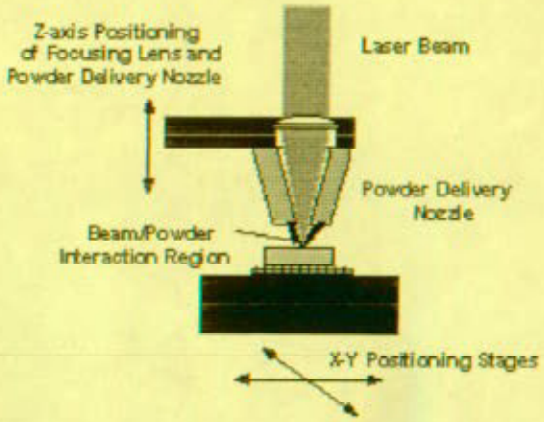

Figure 1: Schematic drawing of the LPD process.

ALLOY 690

Three different Alloy 690 powder chemistries were processed by LPD; PM 690N_2 (0.15% Al and 0.15%Ti with .008 B and 0.12 N), IM 690N_2 (0.3% Al and 0.3%Ti with .002 B and 0.12 N), and IM 690Ar (wrought chemistry with no nitrogen - argon atomized). These three compositions represent the current PM specification (PM 690N_2) the wrought specification (IM 690Ar), and the wrought specification with nitrogen added (IM 690N_2). The PM specification was developed due to poor fabricability (low hot ductility) of powder based IM 690N_2.

Small rectangular (0.5 inch by 2.0 inch by 4.0 inch tall) Alloy 690 specimens were produced by LPD with layer thickness and hatch spacing of 0.02 inch, linear velocity of 30 inches per minute, and Nd:YAG laser fluence of about 400 watts. The LPD processed IM 690N_2 and PM 690N_2 had similar mechanical properties in the as-deposited state, average room temperature yield strengths of 67 ksi and elongation of 46%. The IM 690Ar containing no nitrogen had lower room temperature and elevated temperature (650°F) tensile strength than the other two 690 variants due to the lack of nitrogen. However, the LPD processed IM 690Ar still had very good elevated temperature (650°F) yield strength due to its fine grain size (fine cellular structure). All of the Alloy 690 LPD processed materials were slightly anisotropic with material in the build direction about 10% less in strength and toughness than measured in the direction perpendicular to the build. Mechanical property results from the Alloy 690 LPD variants in the as-deposited condition and taken from the build direction are given in Table 1.

The as-deposited microstructures of the Alloy 690 variants are similar. The typical microstructure, as shown in Figure 2a, is layered with featureless boundaries denoting build passes with epitaxial growth across these layers with large interlayer cell clusters. Figure 2b gives a close up of the interlayer cellular structure. Ultimate tensile strengths (100 ksi) of the as-deposited Alloy 690 variants are lower than the values for wrought by about 10%, most likely due to the absence of grain boundary carbides and large second phase titanium chromium nitrides (Ti, Cr)N that are normally seen in wrought processed IN 690.

Table 1: Mechanical property results from LPD processed variants of Alloy 690.

Process-Alloy	Test Temp (°F)	UTS (ksi)	YS (ksi)	% EL	% RA
LPD-PM 690N_2	RT	100	67	46	69
LPD-PM 690N_2	650	84	54	42	69
LPD-IM 690Ar	RT	89	55	57	70
LPD-IM 690Ar	650	69	45	50	70
LPD-IM 690N_2	RT	107	67	48	65
LPD-IM 690N_2	650	87	54	44	62
HIP-PM 690N_2	RT	118	55	57	58
HIP-PM 690N_2	650	96	44	54	54
IN 690[4] (Annealed)	RT	105	50.5	41	-

Note: The LPD material is in the as-deposited condition (in the build direction). PM 690N_2 data is from HIP'd and rolled, annealed and carbide precipitation treated material.

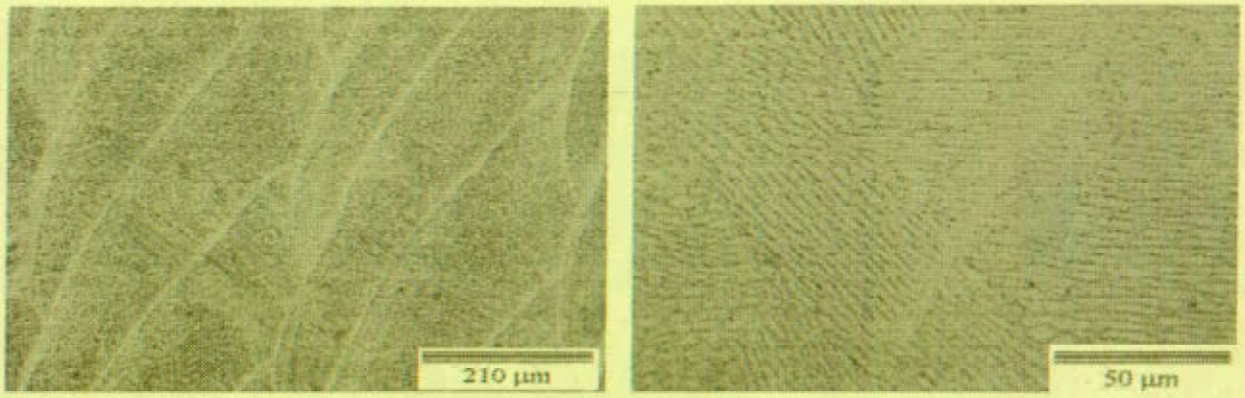

(a) (b)

Figure 2: Optical micrographs of as-deposited LPD PM 690N_2 (a) showing the layering effect from the build passes, and (b) the fundamental cellular structure.

After a heat treatment of 1700°F for one hour the microstructure transforms into irregular grains similar in size to the original cell clusters as shown in Figure 3a. This microstructure is compared to hot isostatic pressed (14.5 ksi at 2065°F for 4 hours) PM 690N_2 in Figure 3b. The LPD grain structure size after heat treatment is on the same scale as the HIP'd material, however the grain boundaries of the LPD material appear much cleaner with no prior particle boundaries.

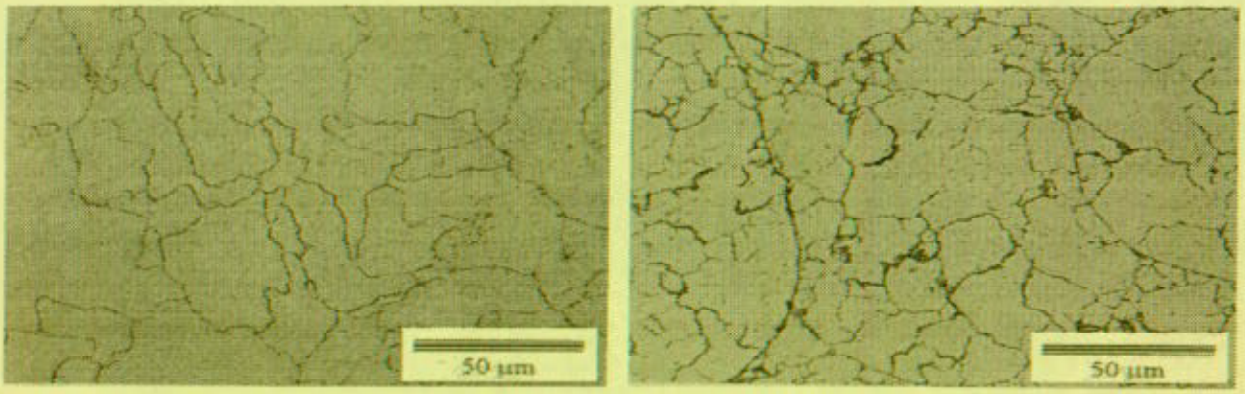

(a) (b)

Figure 3: Optical micrographs (a) heat treated (1700°F for one hour) LPD PM 690N_2. and (b) HIP'd PM 690N_2 (14.5 ksi at 2065°F for 4 hours).

Transmission Electron Microscopy (TEM) of the as-deposited Alloy PM 690N_2 (Figure 4a) reveals only very fine second phase particles. This microstructure was similar for all of the Alloy 690 variants. Heat treatment (1700°F for one hour) caused a fine precipitation of (Ti, Cr)N as shown in Figure 4b.

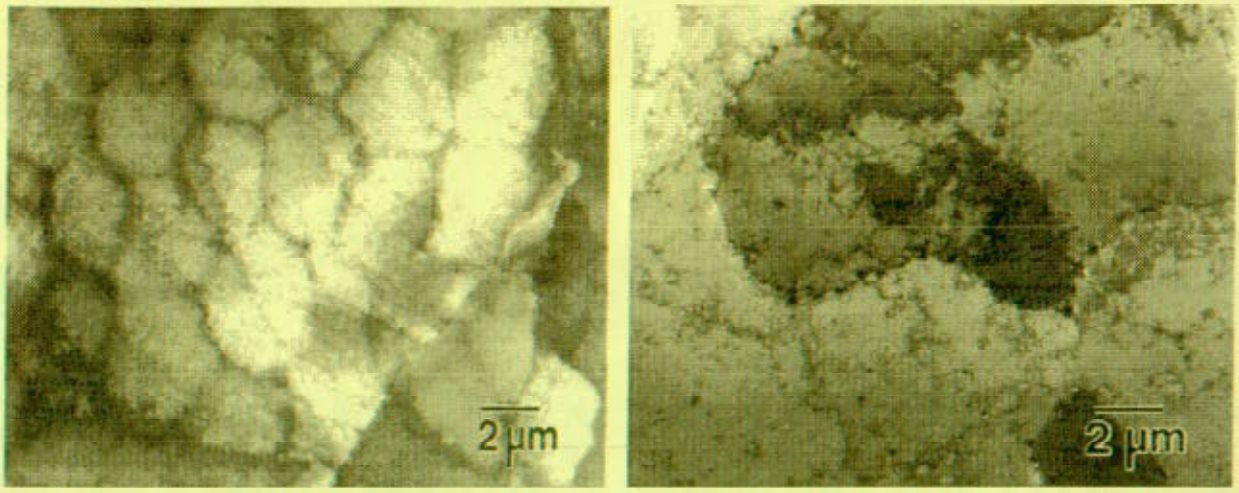

(a) (b)

Figure 4: Transmission Electron Microscopy (TEM) micrographs of LPD PM 690N_2 (a) as-deposited and (b) heat treated (1700°F for one hour), note the presence of the fine (Ti, Cr)N.

The difference in the IM 690Ar from the two nitrogen atomized alloys is the absence of fine (Ti, Cr)N as shown in Figure 5b. The micrograph in Figure 5b also shows the grain boundary carbides that are normal in wrought annealed IN 690.

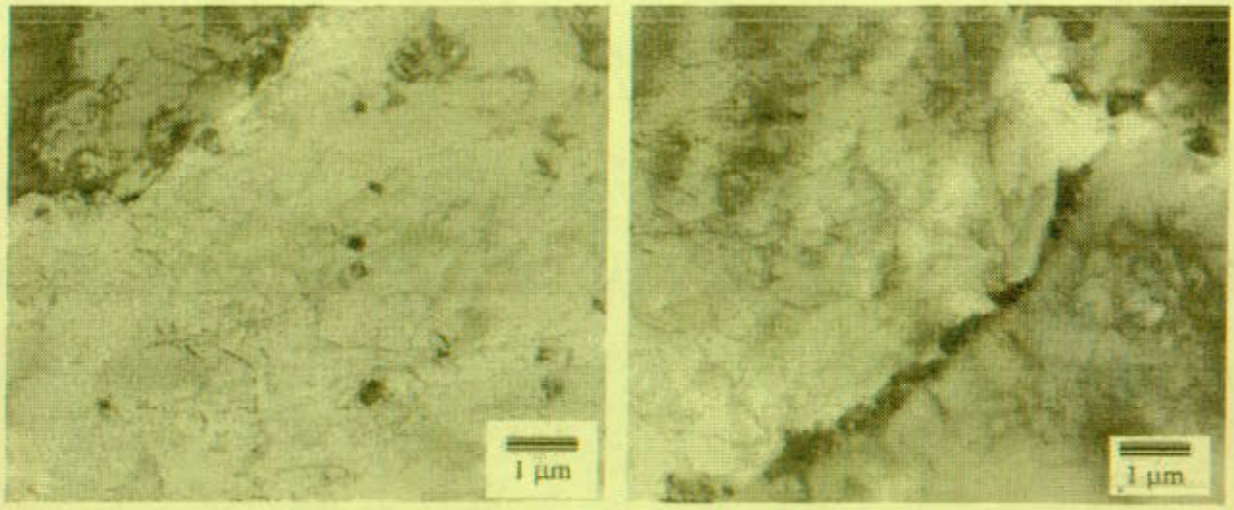

(a) (b)

Figure 5: Transmission Electron Microscopy (TEM) micrographs of heat treated (1700°F for one hour) microstructure of (a) LPD PM 690N_2, and (b) LPD IM 690Ar. Note the absence of second phase particles in the matrix of the heat treated LPD IM 690Ar.

EFFECT OF SPECIFIC ENERGY ON MECHANICAL PROPERTIES

The size of the molten pool has an inverse effect on the cooling (solidification) rate. The effect of the size of the molten pool on the solidification rate will therefore have an effect upon microstructure. High solidification rates lead to finer microstructural features (e.g. grain size) and suppress the formation of

second phases. This produces more homogenous microstructures, and in some cases leads to the formation of metastable phases. Refined microstructures usually result in corresponding improvements in mechanical properties.

Parametric studies were performed to examine property and microstructural variations at different build rates. It is possible to duplicate a solidification rate at different build rates by varying laser power, build thickness, and process linear velocity. For any power level and velocity the build thickness is constrained by the size of the molten pool. Molten pool size is directly proportional to power level and inversely proportional to linear velocity. Build rate is a function of build thickness and linear velocity. If conditions are set where the molten pool size is smaller than that required for the particular build condition, the material will have interconnected porosity due to insufficient pool bead overlap. On the other hand, if the molten pool size is much larger than the build condition warrants, the solidification rate will be slower and metal vaporization will increase and cause condensation to occur on the powder delivery.

Preliminary studies included varying the power level at a constant build rate while producing 0.5 inch diameter Alloy PM 690N_2 rods. When using the same operating parameters on a 1.0 inch square bar the actual build rate increases. As the build area in a layer increases, the actual build rate increases since less time is taken to decelerate and accelerate at the edges of the structure being built. The maximum possible build rate is calculated by Equation (1) below.

$$BR_{\max} = T_{ls} \times T_{hs} \times V_l \times 60 \qquad (1)$$

Where BR_{max} is the maximum possible build rate (cubic inches per hour), T_{ls} is the layer thickness in inches, T_{hs} is the hatch spacing in inches, and V_l is the linear velocity in inches per minute.

RESULTS

Mechanical properties and microstructures of 0.5 inch diameter rods were obtained for various T_{ls}, T_{hs}, V_l, and laser power levels (P_L). The results from this study show that within the range of parameters chosen (See Table 2) the microstructure, 0.2% yield strength (YS), ultimate tensile strength (UTS), percent reduction in area (%RA), and percent elongation (%EL) are not significantly affected. These parameters are not necessarily the optimum operating condition. Material produced at the highest actual build rate (BR_{act}) shows an UTS and % RA decrease. Examination of the microstructures in Figure 6 produced at conditions from Runs E and F show that the material produced during Run F has a slightly finer grain and more uniform structure than the material produced in Run E. This information may lead one to conclude that the material processed in Run F solidified at a faster rate than the material in Run E. Better control over the heat input per unit volume should provide more consistent results.

Table 2: Parameter study results on 0.5 inch diameter Alloy P/M 690N_2 rods.

Run #	T_{ls} (in)	T_{hs} (in)	V_l (in/min)	P_L (watts)	BR_{act} (in^3/hr)	UTS (ksi)	% RA
A	0.015	0.015	35	375	0.24	50.7	59
B	0.020	0.020	35	450	0.54	49.7	61.2
C	0.020	0.020	50	500	0.65	47.8	66.6
D	0.025	0.025	50	575	0.92	50.7	60.8
E	0.025	0.025	75	700	1.11	45.3	38.5
F	0.020	0.020	50	480	0.62	57.3	54.4

Further specimens were prepared at higher build rates and larger surface areas. Build rates up to 3 cubic inches per hour were attempted. Specimens were prepared with surface areas of 2.25, 4.0 and 5.0625 square inches. These specimens were produced using various T_{hs} and T_{ls} as well different V_l as given in Table 3. The mechanical properties of LPD Alloy PM 690N$_2$ are plotted against BR_{max} in Figure 7. There is an abrupt transition above 2.0 cubic inches per hour build rate where the UTS, % RA and % EL decrease.

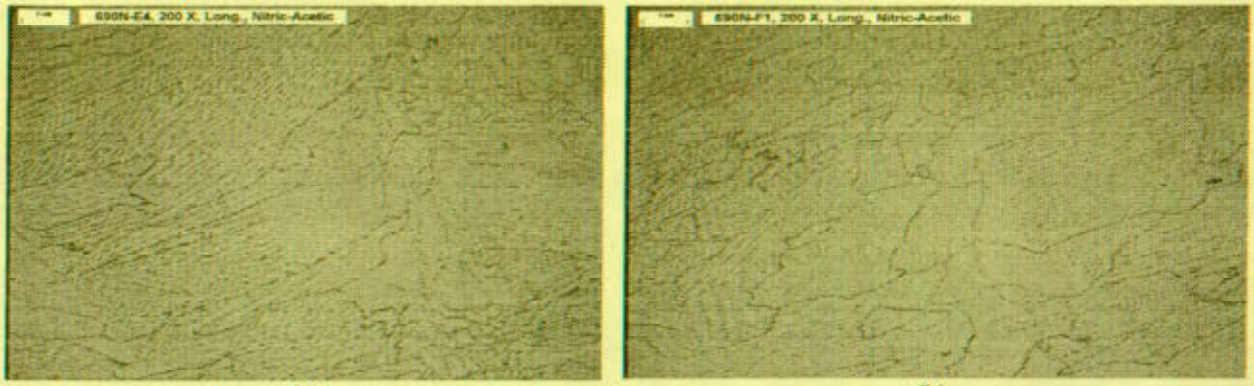

(a) (b)

Figure 6: Microstructures from parameter study on LPD fabricated 0.5 inch diameter Alloy PM 690N$_2$ rods, (a) Run E and (b) Run F.

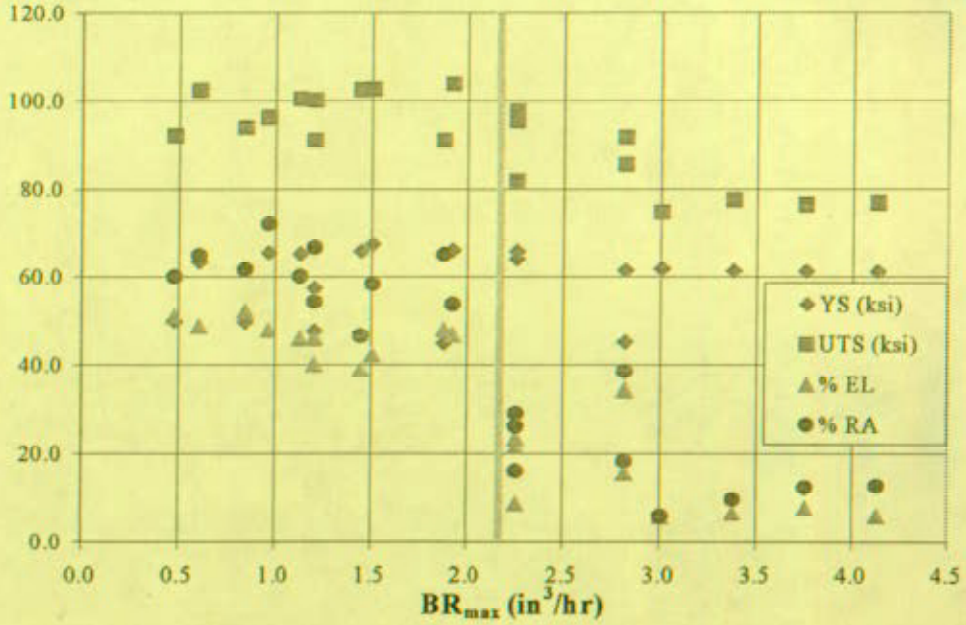

Figure 7: Mechanical Properties of LPD Alloy P/M 690N$_2$ versus build rate .(BR_{max}).

Actual build rates for the LPD Alloy PM 690N$_2$ specimens are plotted as a fraction of maximum possible build rate as calculated by Equation (1) versus layer surface area for varying linear velocities in Figure 8. For lower V_l and larger surface areas the actual build rates approach BR_{max}. At these conditions, the end turn around time losses are low compared to the total build time. As V_l increases over any surface area, the BR_{act} will become a lower fraction of BR_{max}.

Molten pool size is an inverse function of build rate and is directly proportional to absorbed energy. Combining build rate with absorbed energy gives us a term that describes the specific energy (SE) of the

system for all conditions. This term is simply the absorbed energy divided by the BR_{max} as expressed in Equation (2). It is reasonable to use BR_{max} here since, except for decelerations and accelerations at the build line ends, it accurately describes the volume of material being added to the part per unit time. The SE of the system has a direct effect upon the molten pool size and therefore can be used to relate to properties and microstructure. Equation (2) defines the specific energy in the LPD process.

$$SE = \left(\frac{P_L \times \alpha}{BR_{max}} \right). \quad (2)$$

Where SE is the specific energy absorbed in watt-hour per inches cubed, P_L is the emitted laser energy in watts and α is the fraction of laser energy absorbed.

Table 3: Parameter study results on 2.25, 4 and 5.0625 inch square Alloy PM 690N_2 bars.

Run #	Layer Area (in^2)	T_{ls} (in)	T_{hs} (in)	V_l (in /min)	P_L (watts)	BR_{max} (in^3/hr)	BR_{act} (in^3/hr)	% of BR_{max}	UTS (ksi)	% RA
I	2.25	0.025	0.025	60	603	2.25	1.91	0.85	95.4	26.0
J	2.25	0.025	0.025	75	680	2.81	2.25	0.80	85.5	18.3
K	2.25	0.025	0.025	90	756	3.38	2.65	0.78	77.5	9.6
L	4	0.025	0.025	40	603	1.50	1.40	0.93	102.5	58.4
M	4	0.025	0.025	60	660	2.25	1.95	0.87	97.6	28.9
N	4	0.02	0.02	40	508	0.96	0.91	0.95	96.1	72.0
O	4	0.02	0.02	60	565	1.44	1.29	0.90	102.4	46.6
P	4	0.02	0.02	80	641	1.92	1.64	0.85	103.9	53.8
Q	5.0625	0.025	0.025	30	565	1.13	1.11	0.99	100.4	60.1
R	5.0625	0.025	0.025	60	641	2.25	2.06	0.92	81.7	16.1
S	5.0625	0.025	0.025	80	718	3.00	2.53	0.84	74.6	5.8
T	5.0625	0.025	0.025	100	794	3.75	3.04	0.81	76.3	12.3
U	5.0625	0.025	0.025	110	945	4.13	3.14	0.76	76.8	12.7

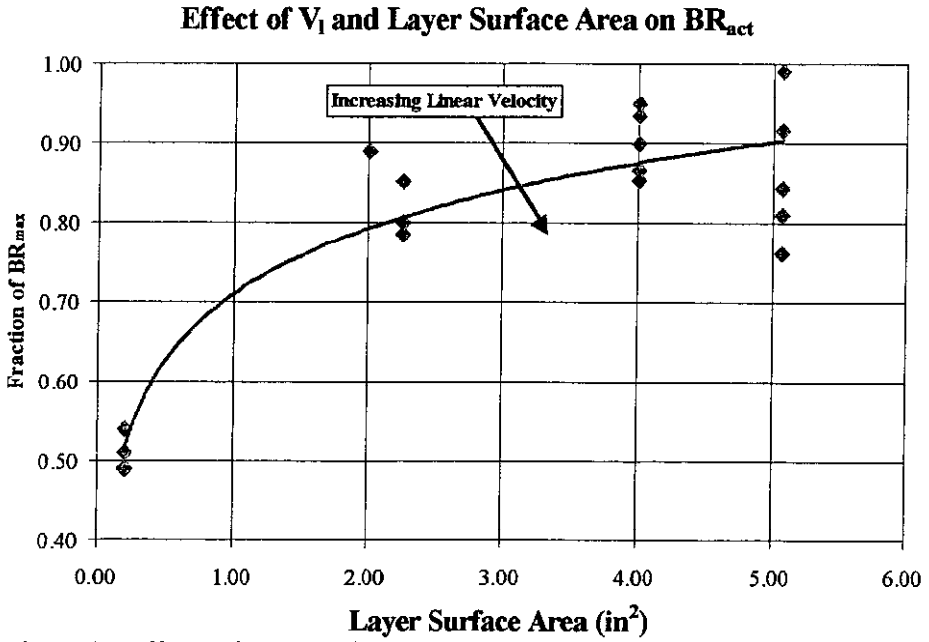

Figure 8: Effects of layer surface area and V_l on BR_{act} as a fraction of BR_{max}.

Maximum build rates were plotted versus specific energy for the LPD PM 690N_2 material in Figure 9. This plot shows that specific energy decreased with increasing build rate. The tensile properties from the LPD Alloy PM 690N_2 bars and rods were also plotted against specific energy in Figure 10. There is a decrease in mechanical properties (ductility and ultimate tensile strength) at about 110 watt-hr/in^3. This specific energy can be considered to be a threshold value for LPD Alloy PM 690N_2 material processing. It happened that all of the specimens built at greater than 2.0 in^3/hr were produced with less than 110 watt-hr/in^3 specific energy.

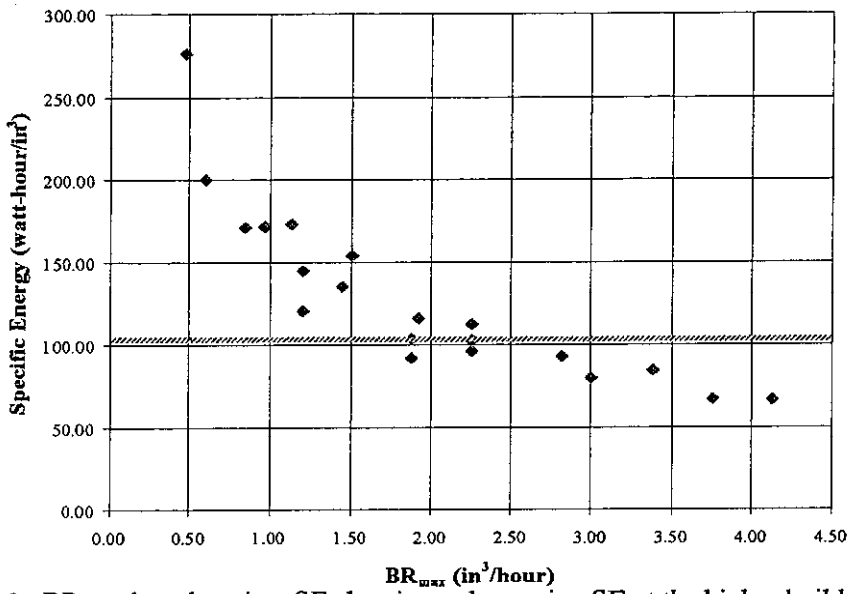

Figure 9: BR_{max} plotted against SE showing a decreasing SE at the higher build rates.

The energy required for heating a unit volume of Alloy 690 from room temperature to melting point plus 200°F superheat (H_{690}) was calculated to be about 40 watt-hour/in^3. It is assumed that bead overlaps of about 30% are required to produce adequate bulk builds. Therefore the specific energy required for bulk builds needs to take into account melting the added and overlap materials and heat losses due to conduction (convection and radiation losses are considered negligible). Based on a flat surface

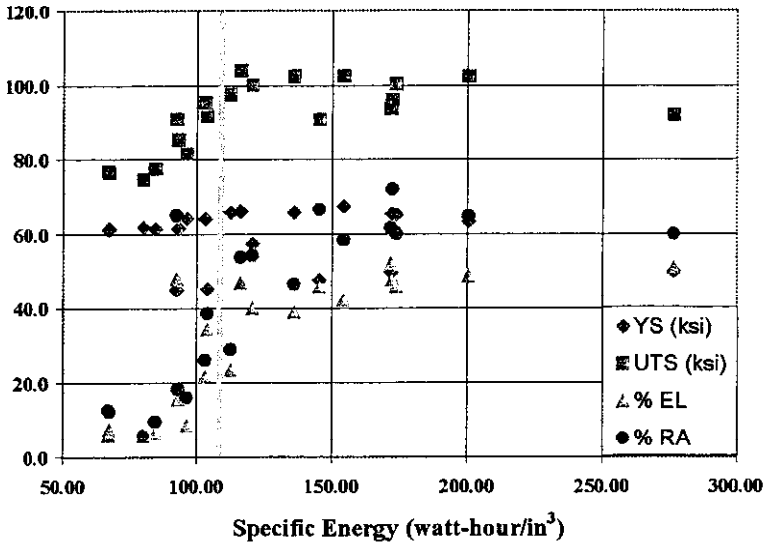

Figure 10: Mechanical properties plotted as a function of SE.

hemispherical melt pool, a geometrical constant multiplier of 2.2 is used to account for melting the deposit and overlap material. Using this multiplier plus a factor for heat conduction of 0.5 gives a good fit between the observed property degradation point for LPD PM $690N_2$ of 110 watt-hr/in^3 and the calculated energy required ($2.2 + .5 = 2.7$, $2.7 \times H_{690} = 108$ watt-hr/in^3). Based on these observations a performance threshold point of 110 watt-hr/in^3 should be used when LPD processing Alloy PM $690N_2$.

A 12 inch diameter LPD Alloy PM $690N_2$ ring, as shown in Figure 11, was fabricated using a 6 kW CO_2 laser operating at a SE of 134 watt-hour/in^3 and build rate of 10 in^3/hour. This ring was therefore produced above the performance threshold point for Alloy PM $690N_2$. The resulting average mechanical properties for this material were found to be 108 ksi - UTS, 67 ksi - YS, 41 - % EL, and 53 - % RA. These properties are consistent with those found at lower LPD build rates when processing at a SE above the performance threshold.

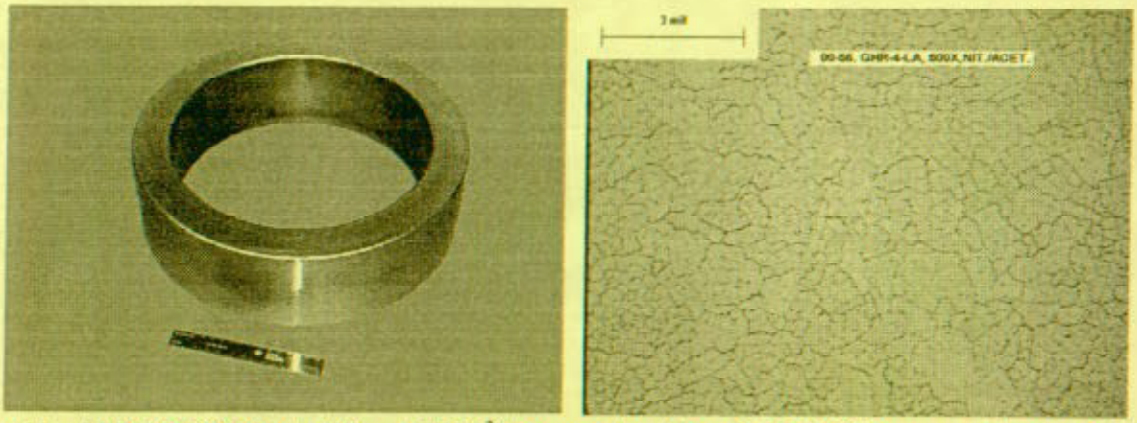

Figure 11: LPD PM $690N_2$ at a BR_{act} of 10 in^3/hour produced by a 6 kW CO_2 laser operating at a SE of 134 watt-hour/in^3, (a) 12 inch diameter ring, 4 inch high and 1.5 inch thick, (b) optical micrograph showing a microstructure similar to that found in lower LPD build rates.

The empirical model for Alloy PM $690N_2$ assumed an absorption constant of 0.3. The value of this constant can be affected by the material reflectivity, laser focus point relative powder impingement point, powder characteristics (size, shape, distribution), and powder flow. The powder cloud formed at the impingement point of the powder jets interacts with the laser beam. The surface material and powder absorbs some of the laser energy, the rest is reflected. The incoming powder also absorbs some of this reflected energy. Therefore the density of the powder cloud has a large effect upon the total energy absorbed during deposition. Increasing the powder cloud density while maintaining a constant mass flow rate should help improve deposition utilization due to increased powder-laser beam interactions.

The other factor that affects this model is the material thermal conductivity. The heat conduction factor used above will be proportional to the thermal conductivity of the material or in the case of cladding the substrate material.

CONCLUSIONS

The necessity to modify chemistry (as in HIP'd powder materials) from normal ingot metallurgy may not be necessary when processing by LPD. The effects of build rate on the mechanical properties of LPD Alloy $690N_2$ were shown to be negligible when specific energy is maintained above an identified performance threshold point. A basic model has been presented for developing fundamental operating parameters for LPD.

ACKNOWLEDGEMENTS

The Nd:YAG laser LPD processing for the Alloy 690 chemistry variants part of this work was prepared at both Los Alamos National Laboratory by Gary Lewis and Sandia National Laboratory by Michelle Griffith. Thierry Marchione performed the CO_2 laser LPD work at Gremada Industries, Inc., West Fargo, North Dakota.

REFERENCES

1 INCONEL – Registered Trademark of INCO Alloys International, Inc.

2 R. Vilar, "Laser Cladding," *International Journal of Powder Metallurgy*, Vol. 37, No. 2, March 2001, pp. 29-48.

3 J.W. Sears, "Direct Laser Powder Deposition - State of the Art", *Powder Materials: Current Research and Industrial Practices*, Proceedings of the 1999 Fall TMS Meeting, ed. by F.D.S. Marquis, November 1999, pp. 213-226.

4 ASM METALS HANDBOOK, Volume 2, Tenth Edition, p.438.